



# The implementation of an easy-to-apply NMR cryoporometric instrument for porous materials

J. Beau W. Webber<sup>a,\*</sup>, Huabing Liu<sup>b</sup>

<sup>a</sup> Lab-Tools Ltd. (nano-science), Marlowe Innovation Centre, Marlowe Way, Ramsgate CT12 6FA, UK

<sup>b</sup> Beijing Limecho Technology Co., Ltd., Beijing 102299, China



## ARTICLE INFO

### Keywords:

Pore-size  
Nmr cryoporometry  
Time-domain  
Nmr relaxation  
Benchtop

## ABSTRACT

Time-domain NMR has been extensively utilised to study various characteristics of fluid-saturated porous materials for instance their mobility, dynamics, stiffness, viscosity and rigidity features, particularly for solid hydrocarbons, rubbers and other polymers. As a unique time-domain technique available for over 30 years, NMR cryoporometry (NMRC) may be used to obtain pore-size distributions of the measured samples. To accurately control the sample temperature, a Peltier thermo-electrically cooled variable temperature probe has been developed and integrated with a highly compact precision NMR time-domain relaxation spectrometer, therefore providing the community with a high-performance instrument for NMR Cryoporometry. To extend the application of aforementioned high-performance NMRC instrument into more scenarios, we designed a series of lightweight, compact and integral models with optional NMR frequencies from 12 MHz up to 23 MHz. The measured sample temperature can be precisely controlled from about  $-60^{\circ}\text{C}$  to  $+80^{\circ}\text{C}$ , with an excellent temperature resolution of 10 mK or better near the probe liquid bulk melting point. Therefore, it offers a fairly wide NMRC pore-size distribution ranging from about 1 nm to 2  $\mu\text{m}$  by using water as the probe liquid in the pores, significantly wider than is possible when applying generic NMR Spectrometers for NMRC. A preliminary example of NMR Cryoporometric measurements on two special cement samples is shown in the paper in which the measured pore scales as well as their repeatability are demonstrated. Furthermore, various nano-materials, such as MOF, zeolite and shale kerogen would be potential materials to study by using these new available NMRC instrument models. We aim to offer this technique as a quantitative and easy-to-apply unitary bench-top tool for an even wider range of porous material.

## 1. Introduction

NMR Cryoporometry (NMRC) [1,2] is, like Gas Adsorption [3], a thermodynamic method of measuring pore size distributions. NMRC can measure pore diameters on a scale from sub-nanometers to over microns.

Gas Adsorption uses the Kelvin Eq. [4], which is the constant-temperature case of the Gibbs Eqs. [5–7], while NMRC uses the Gibbs-Thomson Equation [4,8–10], which is the constant-pressure case. Nano-sizing a crystal (as when it is in a nano-pore) results in a small radius of curvature for the crystal, resulting in an inwardly directed surface tension – which is equivalent to a change to the volumetric Gibbs Free Energy in the crystal [2]. As a result the melting temperature is lowered, compared with the normal bulk melting temperature of the liquid.

For NMRC, a probe liquid is added to the porous material, the sample is cooled until all the liquid in the pores is frozen. The sample is then slowly warmed up. The amplitude of an NMR echo is used to monitor the quantity of the liquid that has melted at a particular temperature. The Gibbs-Thomson transformation is used to convert the melting-point depressions to pore-sizes, and the Strange-Rahman-Smith transformation [1,2] is used to obtain the porosity at the different pore-sizes.

NMRC has many key advantages over both Gas Adsorption and Thermo-porosimetry [11], including that while for pore volume calibration purposes it is advantageous to pre-dry the samples, it is not essential, and can be used, for instance, with samples like wet clays, or hydrogels, whose pore-structure would suffer if pre-dried. Another significant feature is that the probe liquid, as well as water, may be an organic liquid. This can be used to probe the actual effective pore volumes of the pores for a particular liquid [12]. Compared to the difficulty

\* Corresponding author.

E-mail addresses: [Dr.BeauWebber@gmail.com](mailto:Dr.BeauWebber@gmail.com), [nmr@lab-tools.com](mailto:nmr@lab-tools.com) (J.B.W. Webber), [huabing.liu@limecho.com](mailto:huabing.liu@limecho.com) (H. Liu).

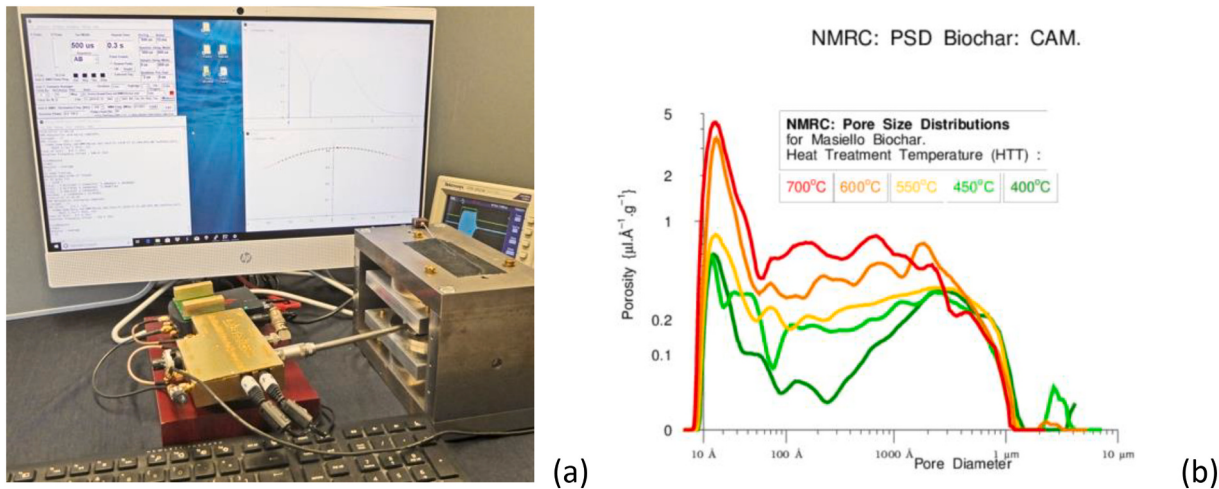


**Fig. 1.** (a) An early NMR Cryoporometer version; (b) NMRC results from five biochars under different thermal treatment.

of accessing porous system saturated by water or other liquids using conventional gas sorption and MIP methods, NMRC has been demonstrated as a friendly technology for soft material research. Another advantage is NMRC is compatible with and freely combinable with any other NMR methods, for instance NMR relaxometry, spin lock and imaging methods, as a multiple-parametric approach. This will allow for an extension of the obtained information to more detailed microscopic or/and spatially-resolved pore-filling fluid distribution.

We offer for general use a lightweight compact integral benchtop NMR Cryoporometer for nanometric to micron pore-size distribution measurement, with a built-in palm-top precision compact time-domain NMR relaxation spectrometer, and graphical user interface.

## 2. NMR Cryoporometry (NMRC) theory

Josiah Willard Gibbs and three different Thomsons (James Thomson, William Thomson (later Lord Kelvin) and J.J. Thomson) applied experiment, thermodynamics and generalised dynamics to produce an equation that well describes the phase-change behaviour of liquids in confined geometry; the Gibbs–Thomson equation for the melting point depression,  $T_m$ , for a small isolated spherical crystal, of diameter  $x$ , in its own liquid, may be expressed as [2]:

$$\Delta T_m = T_m^\infty - T_m(x) = 4\sigma_{sl}T_m^\infty / x\Delta H_f\rho_s$$

A development of the Gibbs–Thomson equation has been discussed that relates these phase changes so that the pore area  $a_p$  and volume  $v_p$  are related to the melting point depression [13–15]:

$$\Delta T_m = T_m - T_m(x) \approx \frac{a_p \sigma_{sl} T_m \cos(\varphi)}{v_p \Delta H_f \rho_s} \approx \frac{k_d \sigma_{sl} T_m}{x \Delta H_f \rho_s}$$

For many purposes this may be simplified so that the pore diameter  $x$  is related to a melting point depression  $\{K\} = T_m - k_{GT}/x$  where we are grouping all the thermodynamic terms into a single constant,  $k_{GT}\{K\}\text{Å}$  - the Gibbs-Thomson coefficient - usually established by experiment [15,16], and then applied, see Fig. 5.

It is important to note that  $k_{GT}$  includes a term dependent on pore geometry, as does the Kelvin equation.  $k_d$  is the geometry term, and is equal to four for a spherical liquid-crystalline interface (conventionally assumed for cylindrical pores).  $T_m$  is the bulk melting point and the other terms are thermodynamic and density terms [2].

Thus the transformation of melting-point depression to pore-size is given by the Gibbs-Thomson equation, while the measurement of the pore volume vs. size distributions is facilitated by differentiating and remapping the melting curve data using the Strange-Rahman-Smith transformation [11]:

$$\frac{dv}{dx} = \frac{k_{GT}}{x^2} \frac{dv}{dT}$$

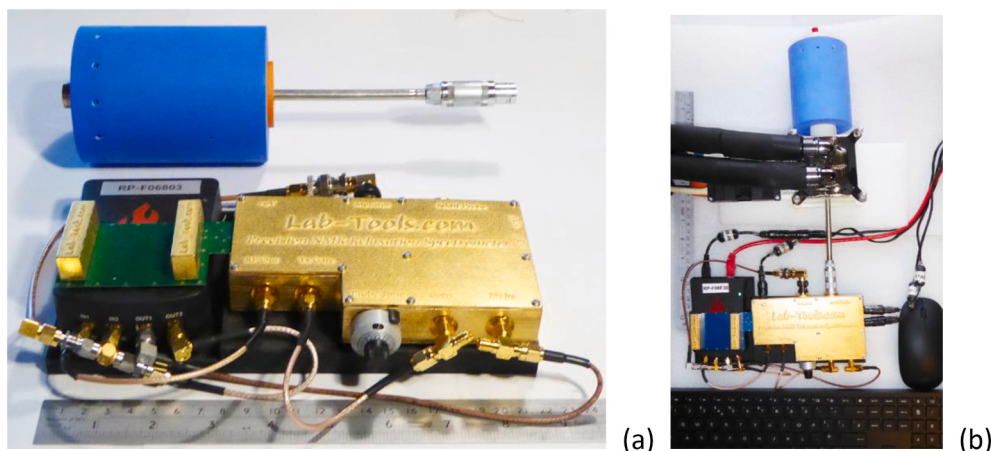


**Fig. 2.** (a) A Lab-Tools time-domain NMR Spectrometer, with Lab-Tools Mandhalas NMR Magnet. (b) The Lab-Tools CryoP4 NMR Cryoporometer (no enclosure), with Lab-Tools blue Mand04 38 mm bore Mandhalas magnet, and Peltier thermo-electrically cooled variable-temperature probe. (For interpretation of the references to colour in this figure legend, the reader is referred to the web version of this article.)

## Lab–Tools NMR Cryoporometer Relational Diagram.

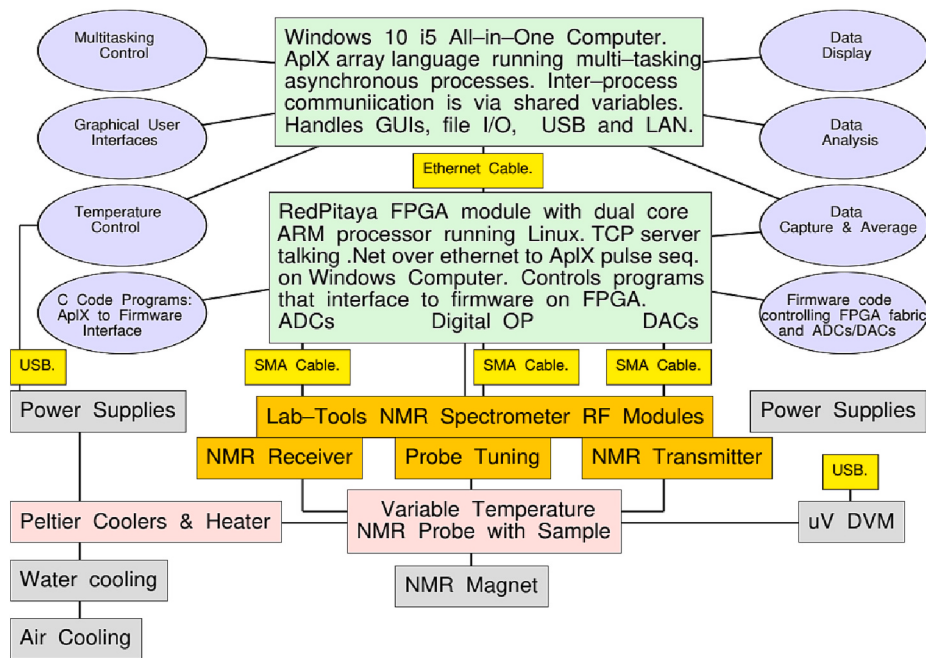


**Fig. 3.** Relational Diagram for Lab-Tools NMR Spectrometer and Cryoporometer.

The Strange-Rahman-Smith equation transforms the quantity of liquid measured at any particular temperature to an incremental pore-volume as a function of pore-size.

### 3. Practical examples of portable NMR Cryoprometers

Previous publications have demonstrated that a wide range of NMRC devices and technologies have been developed. A number of different techniques have been used over the years (1992 to 2021) to vary the temperature of NMRC probes and samples, in which a preferred technique is now to use well-isolated thermo-electric cooling ( $-60\text{ }^{\circ}\text{C}$  to  $+80\text{ }^{\circ}\text{C}$ ), aided to  $-80\text{ }^{\circ}\text{C}$  with gas flow. This gives superb long-term precision of temperature control which is essential for NMR Cryoporometric pore-size-distribution measurements from sub-1 nm to over  $2\text{ }\mu\text{m}$  (10mk control near the liquid bulk melting point). A previous device and its measurement results from five biochars at different states are given in Fig. 1. With the heat treatment temperatures (HTT):  $400\text{ }^{\circ}\text{C}$ ,  $450\text{ }^{\circ}\text{C}$ ,  $550\text{ }^{\circ}\text{C}$ ,  $600\text{ }^{\circ}\text{C}$  and  $700\text{ }^{\circ}\text{C}$ , the samples show increasing pore volumes, in order, as increasing amounts of the labile component are driven off.

With the continuous requirements from new materials research, new fields of application scenarios and the developing information technology, the development of MR equipment tends to be more portable and even miniaturize. To drive forward this technology, both compact Mandhalas and Halbach NMR magnets [17,18] were utilised. The total weight, including the RF Probe, NMR magnet and other necessary parts, is about 3 kg. A laboratory recirculating chiller was set at  $+5\text{ }^{\circ}\text{C}$  to remove waste heat from the thermo-electric cooling head. This gives better isolation from room temperature changes, and the thermo-electric cooling head again gives superb long-term precision of temperature control which is essential for NMR Cryoporometric pore-size-distribution measurements from 2 nm to  $2\text{ }\mu\text{m}$  (10mk stability near the probe liquid bulk melting point). All of this applies this NMR time-domain spectrometer as a high-performance but particularly compact NMRC instrument Fig. 2a,b,4a.

#### 3.1. Peltier cooled variable-temperature NMR probe

For the CryoP4 Peltier cooled Cryoporometer, see Figs. 2b, 4a, cooling is achieved by passing a computer controlled current through a dual-layer Peltier element, that is in contact with a copper plate (with a control thermocouple sensor), which is in turn in contact with a copper cold-finger to the NMR sample. Both 3D printed (lost wax) designs and numerically machined designs have been successfully employed. Waste heat is removed from the Peltier element using a standard CPU water cooling block, using a laboratory re-circulating chiller with fluid set to  $+5\text{C}$ . Both conventional fridge designs and Peltier cooled recirculating chillers have been successfully used. Sample temperatures below  $-40\text{C}$  are reachable.

In CryoP6 Peltier probes, with a Halbach NMR magnet, an additional higher power Peltier element has been used between the dual-layer Peltier element and the water-cooled block, giving a NMR sample temperature of below  $-60\text{C}$ .

Using just Peltier cooling, temperatures at the copper plate down below  $-75\text{C}$  have been achieved, and at the NMR sample down below  $-60\text{C}$ , where there is a sample thermocouple in direct contact with the thin-walled glass NMR sample tube [19].

The key advantages of using the Peltier elements as well as a laboratory chiller are that lower temperatures may be reached; these low temperature sections are buried in an insulated block, and are not passed around the laboratory in thermally lagged pipes; also extremely good thermal control is achieved with negligible cycling or oscillation as is commonly observed in standard chillers (see Section 5 and Fig. 5a, b).

### 4. Software and graphical user interfaces

The NMR Cryoprometers are controlled through three paged dual screens (please see the Graphical Abstract): the NMR Spectrometer Graphical User Interface and its graphs and data tables on the first double page; the temperature measurement and ramp controls on the second, and an Analysis page on the third, that applies the necessary transformations to convert from liquid signal amplitude and temperature to pore-volume and pore-diameter.

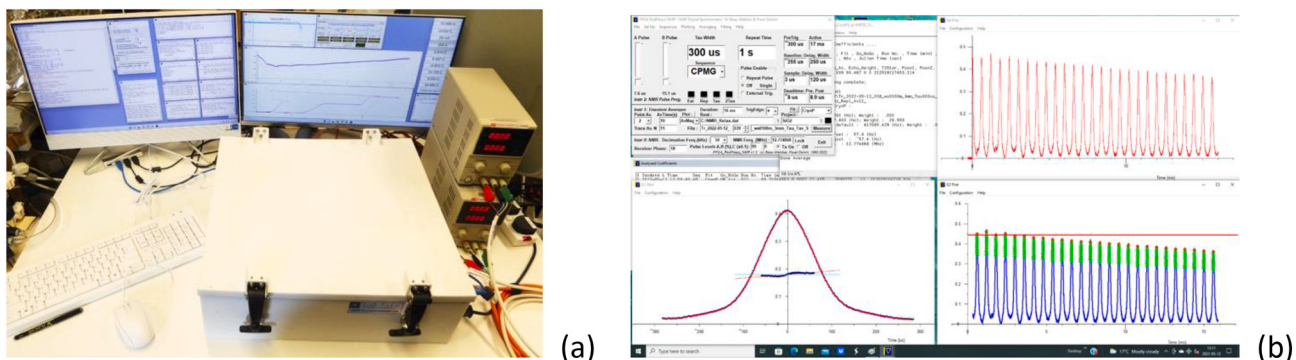


**Fig. 4.** (a) The Lab-Tools CryoP4 NMR Cryoporometer in an enclosure, with HP i5 Windows computer, dual screens and digitally controlled power supplies for the sample Peltier cooler and the heater. (b) The Graphical User Interface (GUI) and the obtained Spin echo and CPMG time domain signals, recording the averaged peak echoes at about 1 ms.

The array processing language Apl is used (AplX by MicroApl), and provides support for array data manipulation, TCP communication to the Dual Linux processors plus Field Programmable Array (FPGA) in the NMR Spectrometer, and the creation and handling of the on-screen Graphical User Interfaces. The FPGA handles the generation of the RF NMR Pulse sequences, under control of AplX. Beside the built-in NMR Sequences, it is possible to specify further sequences in the Apl array language. The FPGA receives the complex digitized NMR signals, does a complex demodulation, and filters and decimates the NMR signals.

The research grade graphical user interface and example traces may be seen in Fig. 4b and the graphical abstract. From the user interface it allows the users to monitor the thermal status at the positions of

sample, RF probe and thermal control unit, as well as modify the pulse sequence parameters and subsequently acquire NMR data.

#### 4.1. Thermal control

For Cryoporometry the temperature control must be excellent, with no temperature reversals. This NMRC instrument offers better than 10mK ° control near the bulk melting points of the probe liquids (See Section 5).

NMRC measurements can last from a couple of hours to 24 h, or even days if a multiple ramp experiment is performed. For this, Peltier cooling is strongly preferred over all the other cooling techniques that have been

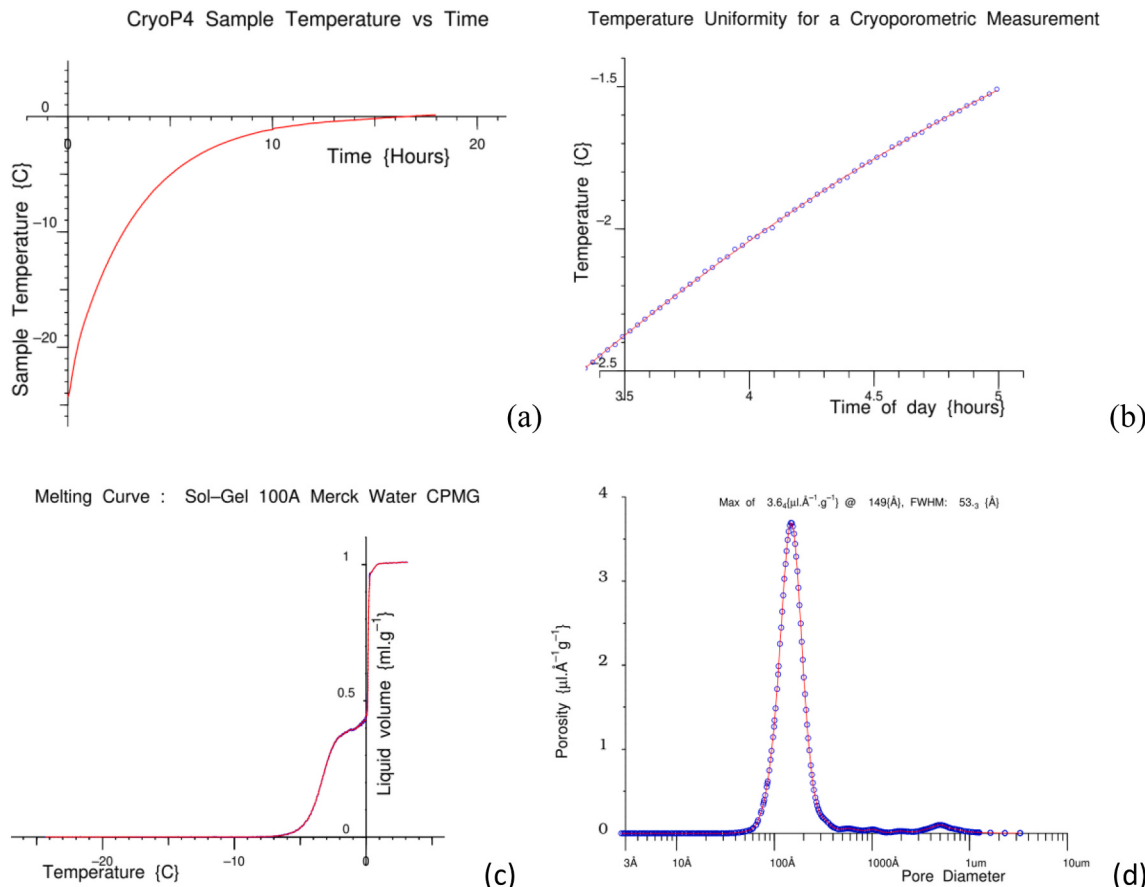
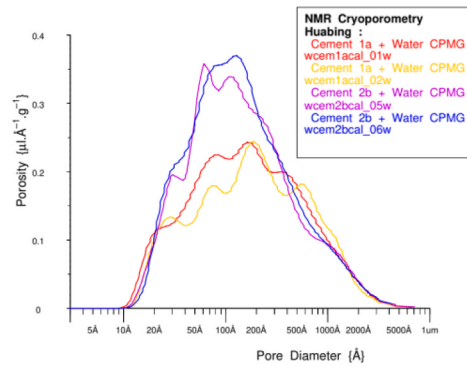


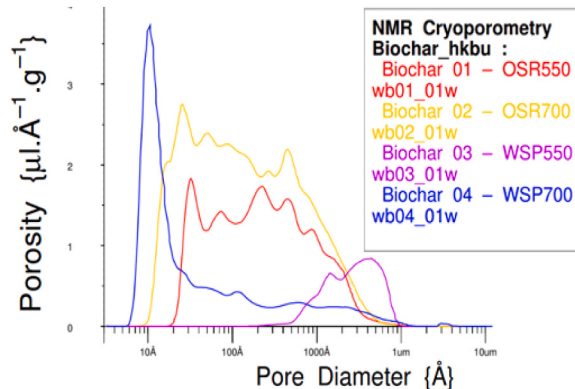
**Fig. 5.** (a) Inverse rate sample warming for a NMRC measurement. (b) Expansion of the region  $-2.5^{\circ}\text{C}$  to  $-1.5^{\circ}\text{C}$  to demonstrate the smoothness of the temperature control. (c) NMR Cryoporometric melting curve for water in a Sol-Gel Silica. (d) Gibbs-Tomson transformed pore-size distribution curve for the Sol-Gel Silica.

## Cement: NMR-C Pore Size Distributions

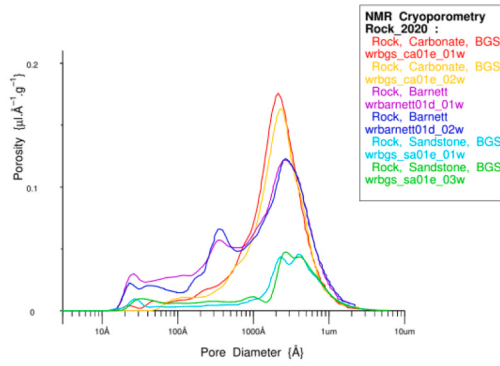


(a)

## Biochar\_hkbu: NMR-C Pore Size Distributions

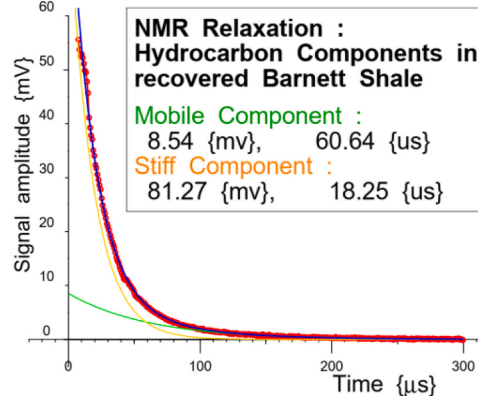


## Rock\_2020: NMR-C Pore Size Distributions



(b)

## Hydrocarbon fractions in Barnett Shale



(c)

(d)

**Fig. 6.** (a) NMR Cryoporometric measurements of pore-size distributions in two pre-prepared cement samples, each measured twice. (b) NMR Cryoporometric measurements of pore-size distributions in porous rocks: a Sandstone, a Carbonate, and a Barnett Shale, each measured twice. (c) NMR Cryoporometric measurements on four Biochar samples with different processing. (d) A two-component exponential fit to the FID from hydrocarbons in a Barnett Shale porous rock sample. Measured data: red dots. The longer more mobile fitted component is the green line, and the shorter more rigid fitted component is the orange line. Their sum is the blue line. (For interpretation of the references to colour in this figure legend, the reader is referred to the web version of this article.)

used in the past, often employing liquid nitrogen.

The sample temperature range is currently from about  $-60^{\circ}\text{C}$  to  $+80^{\circ}\text{C}$ . To achieve this the Peltier and heater currents are precisely controlled from the software (Graphical Abstract and Fig. 3) over the USB via digitally controlled power supplies. The conversion from thermocouple EMF to temperature is facilitated using a 17 part quintic piecewise-polynomial, believed to be good to 1mK over the full range for the Type T thermocouples.

#### 4.2. Implementation of NMR pulse sequences

The Carr-Purcell-Meiboom-Gill (CPMG) echo trains are consecutively obtained at each recovered temperature point. It is worth nothing that this relies on both the fast probe recovery time and precision temperature control. It thus yields suitable NMRC raw data which is Gibbs-Thomson transformed to pore length distributions for the sample. To access more microstructural information, T2 and/or T1 relaxation information may be integrated during the NMRC experiments. From Fig. 4b one may observe that the critical parameters such as pulse length, echo spacing, probe recovery time, dwell time and sampling points, are easily modified to accommodate the individual data acquisition needed for a particular sample.

#### 5. Examples of NMR Cryoporometric measurements on porous materials

Firstly, a simple NMRC measurement on a Sol-Gel silica with a nominal pore diameter of 100 Å (10 nm) is discussed in Fig. 5. The

sample tube is weighed empty, the porous sample is added, weighed, is ideally weighed after drying at 110C, and then sufficient liquid added until there is clearly liquid outside the pores, and the sample re-weighed.

The sample is then cooled until all the signal from an NMR echo (or CPMG echo train) has gone. A linear warming rate can be applied, but for uniform resolution on a logarithmic scale, it is necessary to warm increasingly slowly as the bulk melting point is approached [16, appendix F], Fig. 5a. If we make a quadratic fit (red line) to this warming curve between  $-2.5^{\circ}\text{C}$  and  $-1.5^{\circ}\text{C}$ , one can determine the RMS scatter as 2.3 mK, well within the cited 10 mK, Fig. 5b.

As the sample is warmed up from this all frozen state, Fig. 5c, with initially no amplitude to the echo, significant melting starts at about  $-8^{\circ}\text{C}$ , with the step due to liquid in the pore melting at about  $-4^{\circ}\text{C}$ . There is then a plateau, with little further liquid melting, followed by a step as the bulk liquid melts at about  $0^{\circ}\text{C}$ , followed by a plateau from the signal from the bulk liquid outside the grains. The amplitude of the first plateau gives us the pore volume, and the second plateau gives us (from the total volume of liquid in the sample) the overall volumetric calibration, giving a pore-size distribution, Fig. 5d. This experiment demonstrates that the proposed portable NMRC device, which is much more easy to apply in material analysis, is capable of obtaining the micro-structural information as precise as the standard ones we had provided.

More work has been conducted on different types of porous materials with different pore length structures and features. These example results are given in Fig. 6. Fig. 6(a) depicts the pore size distribution measured from two cement samples. By measuring each sample twice a good estimate of the repeatability of the NMRC measurements can be obtained. Similar experiments were performed on rock sample with different

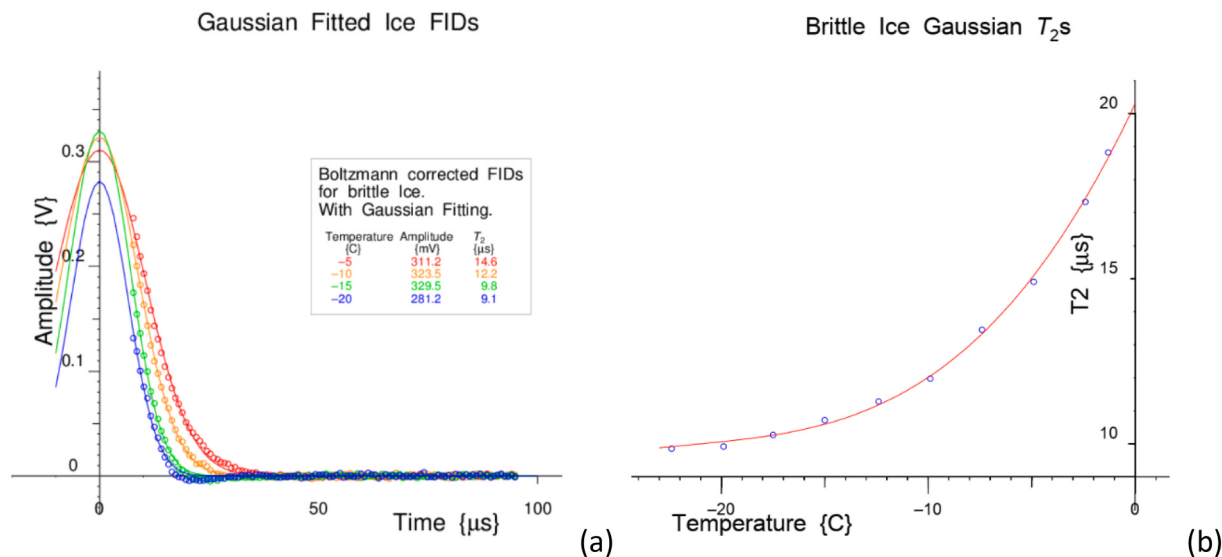


**Fig. 7.** (a) A set of NMR Free Induction Decay Gaussian  $T_2$  measurements on Brittle ice, as a function of temperature. (b) The measured Gaussian  $T_2$ s, showing molecular mobility changes as a function of temperature.

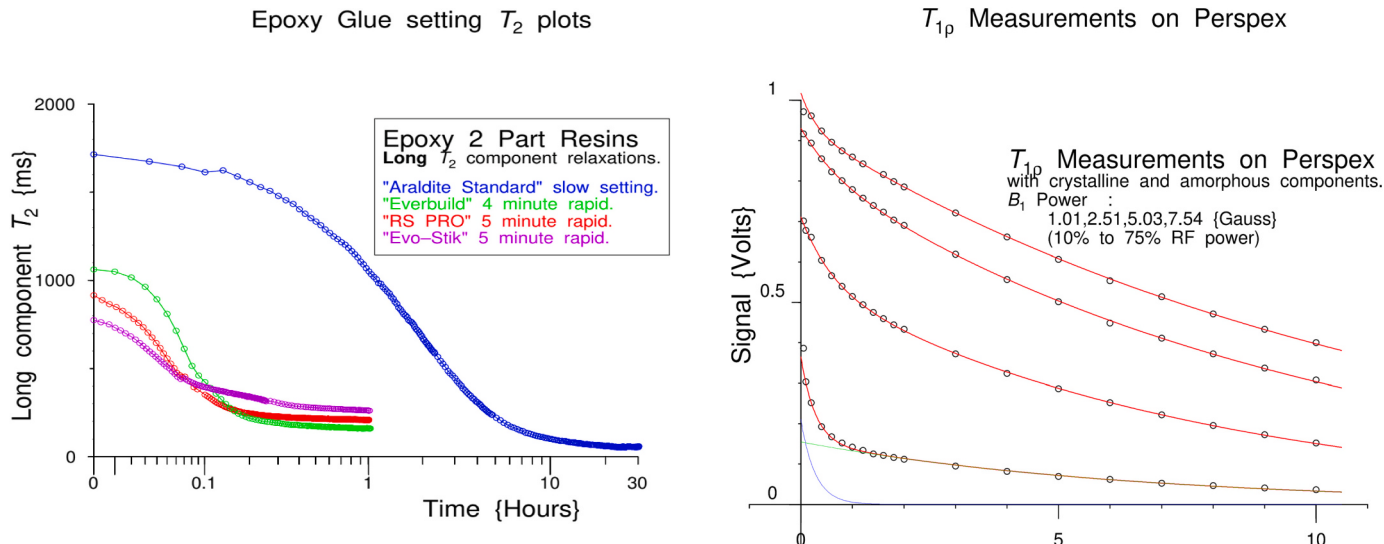


**Fig. 8.** Changes in polymer mobility due to chemical reactions can also be studied. Here we examine four different epoxy resins, as they react and set.

lithologies. The results are shown in Fig. 6(b). Besides the reliable repeatability of the device performance, the results give direct indication of the pore structure in different rock types Fig. 6(d). Moreover, with the cooled variable-temperature probe giving excellent thermal control and therefore uniform sample temperature, the portable NMRC device yields an upper pore-size resolution which extends to about 1 μm.

Some data were measured on four biochar samples using the prototype of this Cryoporometer and the results are shown in Fig. 6(c). The biochar was derived from oilseed rape (OSR) and mixed softwood pellets (SWP) containing 5:95 pine: spruce, from the United Kingdom Biochar Research Centre (UKBRC) Edinburgh. It was pyrolyzed in a pilot-scale rotary kiln unit, at 550 °C and 700 °C.

Fig. 6(d) Shows the FID of hydrocarbons in a dried porous shale, fitted with a double exponential, for which the fast recovery of the NMR receiver is important. The first short component is indicative of a tar-like component on the pore walls; the longer component of a more mobile organic component in the body of the pores.

**Fig. 9.**  $T_{1p}$  measurements of local molecular motion in Perspex, at room temperature, as a function of spin lock time, at 4 different  $B_1$  field strengths 1.1 G, 2.41 G, 5.03 G and 7.54 G (by changing the percentage of linear RF power).

## 6. NMR materials-science measurements as a function of temperature and sample properties

As well as being a high-performance NMR Cryoporometer for measuring nanopores, this instrument can also be very convenient for standard NMR measurements as a function of sample temperature.

With a temperature range currently about from -60 °C to +80 °C, this is very convenient for many material-science investigations, including properties that are often in different disciplines described as mobility, dynamics, stiffness, viscosity or rigidity.

In Fig. 7 we have made  $T_2$  measurement to examine the molecular mobility changes in bulk brittle ice, over a temperature range from -20 °C to just under the bulk melting point of the ice:

Fig. 8 shows some typical measurements monitoring the setting of two-part epoxy resins over more than a day, measuring the changes in the motion of the molecules in the polymers as the setting process

**Table 1**

Double-exponential fitted parameters to the measured Perspex T1ps for the four RF B<sub>1</sub> powers.

Percent Power	RF B <sub>1</sub> {Gauss}	Short Amplitude {mv}	Short relaxation {us}	Long Amplitude {mv}	Long relaxation {ms}
10	1.01	210.8	277.18	154.9	6.5
25	2.51	163.2	619.67	548.2	7.75
50	5.03	95.7	698.21	835.4	9.88
75	7.74	86.3	305.13	931.1	11.74

proceeds and the resins become more rigid.

## 7. Local field fluctuations, as measured by T<sub>1ρ</sub> NMR sequences

As well as having built-in sequences for measuring T<sub>1</sub> and T<sub>2</sub> relaxation times, this spectrometer has NMR sequences for measuring T<sub>1</sub> in the rotating frame (T<sub>1ρ</sub>) at different RF powers (different B<sub>1</sub> strengths), where long RF pulses are used to spin-lock the rotating NMR vector. The T<sub>1ρ</sub> protocol may be combined with NMR Cryoporometric measurements.

The effectiveness of the spin-locking is dependent on the ratio of the strength of the rotating R.F. field B<sub>1</sub>, to the local fluctuating field in the sample. The behaviour as a function of temperature is dependent on whether we are above or below the T<sub>1ρ</sub> minimum. In Fig. 9 we see T<sub>1ρ</sub> measurements made at room temperature on Perspex.

The parameters of the double-exponential fitted curves (in red in Fig. 9) are shown in Table 1, for the four RF B<sub>1</sub> powers. The short component fraction is only about 10% at maximum power, but increases at lower powers, presumably as at these powers it is not as spin-locked. This is indicative of the local B<sub>1</sub> fields in the sample. For the lowest power the short component is plotted in blue in Fig. 9. This data was analysed using the NMR Spectrometer GUI in off-line mode.

## 8. Conclusion

NMRC has been continuously developed and utilised in porous materials research for nearly three decades. The process of NMR cryoporometry involves no material transfer but is local in character, therefore the melting behaviour can provide pore information that is insensitive to constrictions and pore inter-connectivity.

In this paper, a more portable NMRC version combining light-weight Halbach magnet and credit-card size spectrometer was introduced. This version has been successfully utilised to study the pore length scales of different types of porous materials, in which its reliability and reputability has been well proven. Moreover, with this highly reliable variable-temperature unit, this version allows one to study the material

properties as a function of sample temperature. Further NMRC experiments integrating with T<sub>2</sub> and T<sub>1ρ</sub> measurements proves it is even feasible for this proposed portable NMRC instrument to couple with other NMR techniques, which potentially broadens its application scenarios in porous materials.

## CRediT authorship contribution statement

**J. Beau W. Webber:** Conceptualization, Methodology, Software.  
**Huabing Liu:** Conceptualization.

## References

- [1] Strange J, Rahman M, Smith E. Characterisation of porous solids by NMR. *Phys Rev Lett* 1993;71:3589–91.
- [2] Mitchell J, Webber J, Strange J. Nuclear magnetic resonance cryoporometry. *Phys Rep* 2008;461:1–36.
- [3] Brunauer S, Emmett P, Teller E. Adsorption of gases in multimolecular layers. *J Am Chem Soc* 1938;60:309–19.
- [4] Thomson W. On the equilibrium of vapour at a curved surface of liquid. *Phil Mag Series* 1871;4(42) (488–452).
- [5] Gibbs J. On the equilibrium of heterogeneous substances. *Trans Connecticut Acad III* 1875, 1878;108–248:343–524.
- [6] Gibbs J. The Scientific Papers of J.Willard Gibbs, Volume 1: Thermodynamics. New York, London: Dover Publications, Inc., Constable and Co.; 1961. new dover edition, 1906 reprinted.
- [7] Gibbs J. Collected Works. New York: Longmans, Green and Co.; 1928.
- [8] Thomson J. Theoretical considerations on the effect of pressure in lowering the freezing point of waterxvi. Edinburgh: Trans. Roy. Soc.; 1849. p. 575–80.
- [9] Thomson J. On crystallization and liquefaction, as influenced by stresses tending to change form in the crystals. *Proc Roy Soc* 1862;xi:473–81.
- [10] Thomson JJ. Application of dynamics to physics and Chemistry. London: Macmillan & Co; 1888.
- [11] Gane P, Ridgway C, Lehtinen E, Valiullin R, Furo I, Schoelkopf J, et al. Comparison of NMR cryoporometry, mercury intrusion porosimetry, and dsc thermoporosimetry in characterizing pore size distributions of compressed finely ground calcium carbonate structures. *Indust Eng Chem Res* 2004;43:7920–7.
- [12] Webber JBW. Accessible catalyst pore volumes, for water and organic liquids, as probed by nmr cryoporometry. diffusion-fundamentals.org 2014;22:1–8.
- [13] Webber J. A generalisation of the thermoporosimetry Gibbs-Thomson equation for arbitrary pore geometry. *Magn Reson Imaging* 2003;21:428.
- [14] Webber JBW, Dore JC, Strange JH, Anderson R, Tohid B. Plastic ice in confined geometry: the evidence from neutron diffraction and NMR relaxation. *J Phys Condens Matter* 2007;19:415117 (12pp).
- [15] Webber JBW. Studies of nano-structured liquids in confined geometry and at surfaces. *Prog Nucl Mag Res Sp* 2010;56:78–93.
- [16] Webber JBW. The Characterisation of Porous Media. UK: University of Kent at Canterbury; 2000.
- [17] Halbach K. Design of permanent multipole magnets with oriented rare earth cobalt material. *Nuclear Instrum Meth* 1980;169:1–10.
- [18] Raich H, Bluemler P. Design and construction of a dipolar halbach array with a homogeneous field from identical bar magnets: Nmr mandhalas. *Concepts Mag Reson B Magn Reson Eng* 2004;23B:16–25.
- [19] Webber, J.B.W. Webber, patent no.: US 9,810,750 B2, Nov 7, 2017. Nuclear magnetic resonance probes. Application no.: 14/316,409 filed : Jun. 26, 2014. Patent, 2014, 2017.